Int. J. Heat Mass Transfer. Vol. 27, No. 8, pp. 1157 1169, 1984
Printed in Great Britain

0017 9310/84 $3.00 + 0.00

COMPARISON OF STEFAN MODEL WITH TWO-PHASE MODEL OF COAL DRYING

R. W. LYCZKOWSKI
Argonne National Laboratory, Components Technology Division, 9700 South Cass Avenue, Argonne, IL 60439, U.S.A.

and

Y.-T. CHAO
Illinois Institute of Technology, Department of Gas Engineering, Chicago, IL 60616, U.S.A.

(*Received* 15 *March* 1983 *and in revised form* 11 *October* 1983)

Abstract—The Stefan model has frequently been proposed to describe highly non-isothermal rapid drying of porous media. In particular it has been used to analyze the drying of Western coals and lignites which contain up to 40% water, almost all of which is unbound. The Stefan model may be appropriate for freezing processes but may break down when describing processes where much steam is produced within the moist porous material and flows outward because of an internally generated pressure build up. Recently, the first author developed a mechanistic moisture dynamics model called the two-phase model to remedy this deficiency and, thus, to rationally extend the drying theory. The objectives of this paper are: (1) to compare the Stefan and two-phase drying models by analyzing lignite block pyrolysis and subbituminous coal drying experiments; and (2) to determine the range of heating rates for which the Stefan model is adequate. This paper is, to our knowledge, the first to quantitatively assess the adequacy of the Stefan model to describe coal drying.

NOMENCLATURE

C_{pg} heat capacity of vapor at constant pressure [J kg^{-1} K^{-1}]
C_{pl} heat capacity of liquid at constant pressure [J kg^{-1} K^{-1}]
C_{pm} mean heat capacity defined by equation (24) [J kg^{-1} K^{-1}]
C_{pw} heat capacity of dry coal [J kg^{-1} K^{-1}]
h_v scale factor
ΔH_v heat of vaporization (>0) [J kg^{-1}]
j nodal index
K_e effective thermal conductivity [W m^{-1} K^{-1}]
K_{ec} effective thermal conductivity in wet coal region [W m^{-1} K^{-1}]
K_{ed} effective thermal conductivity in dry coal region [W m^{-1} K^{-1}]
K_g permeability [m^2]
$\dot{m}$ total rate of vapor generation per unit pore control volume [kg m^{-3} s^{-1}]
n outward drawn normal direction
P pressure [Pa]
t time [s]
T temperature [°C]
T_i initial temperature [°C]
T_{vap} vaporization temperature [°C]
Δt time interval [s]
V^g local steam velocity [m s^{-1}]
x distance [m]
$\bar{x}$ drying front location [m]
Δx distance interval [m].

Greek symbols
α thermal diffusivity [m^2 s^{-1}]
α_g vapor volume fraction in pores
α_l liquid volume fraction in pores
ε porosity
ε_w volume fraction of solid
μ_g vapor viscosity [Pa s]
ρ mean density, $\alpha_g\rho_g+\alpha_l\rho_l$ [kg m^{-3}]
ρ_g density of vapor [kg m^{-3}]
ρ_l density of liquid [kg m^{-3}]
ρ_w density of dry coal [kg m^{-3}]
ρ_{wo} initial moisture density [kg m^{-3}].

1. INTRODUCTION

THE ECONOMICAL, safe, and environmentally acceptable operation of underground coal conversion (UCC) processes requires predictable and stable operation as well as optimized resource recovery. Water plays an important role in UCC. Detailed fundamental modeling of moisture dynamics (drying and processes associated with drying) is the key to understanding reverse combustion permeability enhancement, monolithic coal block gasification, spalling, subsidence, and water influx and control.

The water contained in coal can be classified as unbound, weakly bound, and chemically bound. Unbound water is driven off at a temperature corresponding to the local saturation temperature (95–100°C at ~1 atm). Weakly bound water is held by absorption, Van der Waals' forces and capillarity and evolves at somewhat higher temperatures. Chemically bound water which resembles water of hydration for crystals is driven off at a much higher temperature typically 200–400°C. Western coals and lignites contain up to 40% water, almost all of which is of the unbound type [1].

Drying modeling is an interdisciplinary science of

importance in chemical engineering, mechanical engineering, soil mechanics, and geoscience. Four models which have won general recognition in the past in interpreting the drying phenomena, according to Tsang and Edgar [2] are: (1) the diffusion theory; (2) the capillary flow theory; (3) the evaporation–condensation mechanism; and (4) simultaneous energy and moisture transfer in porous media. Each model designates a different driving force of moisture movement. Van Arsdel [3], Peck *et al.* [4] and Whitaker [5] have given excellent surveys on the historical development of drying theories and models.

For highly non-isothermal rapid drying of a porous media, the situation is very complicated and the whole process is not well understood. Recently, several models have been formulated. The difference between these models depends on their definition of the evaporation term, the dominating mechanism by which the model is formulated. Tsang and Edgar [2] have a very good survey on these models. Recently, Lyczkowski [6] developed a mechanistic moisture dynamics model called the two-phase model by a straightforward but unique application of recent two-fluid, two-phase flow theory to drying. Included is also an extensive literature review of relevant drying literature and the relationship of the two-phase model to previous models. In the two-phase model, all the liquid and vaporous water are assumed to exist only within the micropores and macropores that are distributed throughout the coal. Thus, no liquid or vapor exists within the ultimate solid portions of the coal itself. This is similar to that taken by Whitaker who uses local volume-averaging [5].

The Stefan model has frequently been proposed to describe rapid drying processes [7]. However, the validity of this model has not been determined by comparison with the more mechanistic two-phase model. The Stefan model may be appropriate for freezing processes but may break down for drying processes where a lot of steam is produced within the moist porous material and flows outward because of an internally generated pressure build up.

The objectives of this paper are to:

(1) numerically solve the two models (two-phase and Stefan) describing the one-dimensional (1-D) drying of moist coal in Cartesian and axi-symmetric cylindrical coordinates;

(2) compare the two models by analyzing Westmoreland and Dickerson's [8] lignite block pyrolysis and Kashiwa and Harlow's [9] subbituminous coal drying experiments;

(3) determine the range of heating for which the Stefan model is adequate by comparing the results with the two-phase model.

This study is, to our knowledge, the first to quantitatively assess the adequacy of the Stefan model to describe coal drying. The results have broad applicability to UCC processes, coal mine fire research, large coal particle gasification, wood pyrolysis, oil shale extraction, pellet drying, and sand mold casting.

2. THE STEFAN MODEL

Transient heat transfer problems involving melting or solidification generally referred to as 'phase change' or 'moving boundary' problems are important in many engineering applications such as the freezing of food, fractional crystallization, and the solidification of metals in sand molds. Solutions of such problems are inherently difficult because the interface between the solid and liquid phases is moving as the latent heat is absorbed or released at the interface. As a result, the location of the solid–liquid interface is not known *a priori* but must be obtained as part of the solution. This is known as a Stefan problem [10]. It has been applied to drying but with little or no justifications [7]. The model is now briefly reviewed.

Consider the evaporation of a single component liquid contained in the pores of a 1-D solid. Heat is assumed to be added continuously at the surface $x = 0$. Prior to the start of drying, the temperature distribution within the solid–liquid mixture will be assumed to be determined by the conventional heat-conduction equation alone if the temperatures are equal locally. After the initiation of drying, the analysis requires the formation of a gas–liquid boundary which moves in the positive x-direction. Figure 1 shows a schematic representation of the process and shows the position of the gas–liquid interface $\bar{x}(t)$ during the drying process. Saturated coal is initially at a temperature T_i and the surrounding temperature is T_0. The heated surface at $x = 0$ is represented by a prescribed time-dependent surface temperature [8, 9]. The mathematical formulation of the problem of drying is as follows

$$\rho C_{pm} \frac{\partial T}{\partial t} = \frac{1}{h_v} \frac{\partial}{\partial n} \left(h_v K_e \frac{\partial T}{\partial n} \right), \tag{1}$$

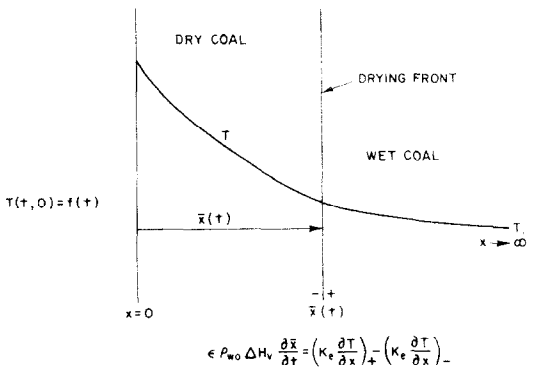

FIG. 1. Schematic representation of the coal drying process described by the Stefan model.

where

h_v = scale factor

$$= \begin{cases} 1 \text{ Cartesian coordinate,} \\ r \text{ axi-symmetric cylindrical coordinate,} \end{cases}$$

and $\partial/\partial n$ denotes differentiation along the outward drawn normal direction. The initial and boundary conditions are given by

$$\text{I.C.:} \quad T(0, x) = T_i, \tag{2}$$

$$\text{B.C.1:} \quad T(t, \infty) = T_i, \tag{3}$$

$$\text{B.C.2:} \quad T(t, 0) = f(t). \tag{4}$$

At the drying front

$$\varepsilon \rho_{w0} \Delta H_v \frac{\partial \bar{x}}{\partial t} = \left(K_e \frac{\partial T}{\partial n} \right)_+ - \left(K_e \frac{\partial T}{\partial n} \right)_-, \tag{5}$$

$$T = T_{vap}, \quad x = \bar{x}(t). \tag{6}$$

The boundary conditions at the drying front are governed by equations (5) and (6) as discussed in Carslaw and Jaeger [10] for freezing problems and were extended to drying of porous materials by Cross *et al.* [7]. The assumptions which enable us to use these equations are that a coal–water or a coal–steam mixture behaves as a single effective component and that steam motion is neglected. We denote the thermal conductivity of the wet coal–water mixture by an effective thermal conductivity K_e^+ and for the dry coal–steam mixture by K_e^-. These may be determined experimentally.

The existence of a moving boundary poses numerical difficulties which have limited most investigations to 1-D problems. Murray and Landis [11] developed two difference schemes to obtain accurate numerical results. Springer and Olson [12] used a finite-difference scheme similar to one of the methods proposed by Murray and Landis [11]. Lazaridis [13] extended it to the multidimensional melting problem. Recently, Yuen and Kleinman [14] developed a numerical scheme using a variable time step finite-difference method. All these methods produce satisfactory agreement with experimental results and analytical solutions for melting or freezing problems. However, they may break down when applied to drying processes where steam is produced within the moist porous material and flows outward because of an internally generated pressure.

Equations (1)–(6) were solved numerically using Springer and Olson's method [12]. More details may be found in Chao [15]. Programming was checked for correctness and accuracy by comparing with an analytical solution for the case of constant temperature at $x = 0$ in Fig. 1 and the semi-infinite solid initially at its melting temperature, T_m [10].

At time $t = 0$, the temperature of the boundary surface at $x = 0$ is raised to T_0, which is higher than T_m and maintained at T_0 for time $t > 0$. As a result, melting starts at the surface $x = 0$ and the solid–liquid interface moves in the positive x-direction. The solid phase being at a constant temperature T_m throughout, the temperature is unknown only in the liquid phase.

From Carslaw and Jaeger [10], the melting front position for this Stefan problem can be evaluated analytically from

$$\bar{x}(t) = 2\lambda(\alpha t)^{1/2}, \tag{7}$$

where λ is the root of

$$\lambda \, e^{\lambda^2} \operatorname{erf}(\lambda) = \frac{C_p(T_0 - T_m)}{L\sqrt{\pi}}. \tag{8}$$

Some physical properties are taken from Murray and Landis [11]:

α = diffusivity of liquid and solid = 2.5808×10^{-5} m^2 s^{-1}
L = latent heat of fusion = 1.162×10^{-5} m^2 s^{-1}
K_e = conductivity of solid and liquid = 86.49 W m^{-1} K^{-1}
C_p = specific heat of solid and liquid = 4.184×10^2 J kg^{-1} K^{-1}
ρ_s = density of solid and liquid = 8.0×10^3 kg m^{-3}
$T_i = T_m = 0$°C
T_0 = 111 K + T_i.

By substituting these physical properties into equation (8), we obtain

$$\lambda \, e^{\lambda^2} \operatorname{erf}(\lambda) = \frac{(4.184 \times 10^2)111}{(1.162 \times 10^5)\sqrt{\pi}} = 0.255. \tag{9}$$

From Curve I of Carslaw and Jaeger [10, p. 287] we can read $\lambda \approx 0.44$. Thus

$$\bar{x}(t) = 4.47 \times 10^{-3}\sqrt{t} \text{ [m]}. \tag{10}$$

This problem was calculated numerically with the same physical properties. It is well known that the stability criterion for the diffusion equation using the explicit finite-difference method is $(\alpha \Delta t)/(\Delta x)^2 \leqslant \frac{1}{2}$. In our calculations, we follow this criterion using $(\alpha \Delta t)/(\Delta x)^2 = 0.2$. Figure 2 compares the melting front position vs time obtained numerically with the analytical solution. From these comparisons, we conclude that the numerical scheme is stable and convergent.

3. THE TWO-PHASE MODEL

Lyczkowski [6] developed a mechanistic theory for drying of porous media by using two-fluid, two-phase flow theory. The model rationally extends classical drying theory to handle rapid drying of moist solids where the bulk motion of steam and water occurs within the matrix. As discussed by Lyczkowski [6], the minimum realistic two-phase drying model is given by:

vapor continuity

$$\frac{\partial}{\partial x} [(1 - \varepsilon_w)\alpha_g \rho_g V^g] = (1 - \varepsilon_w)\dot{m}, \tag{11a}$$

where

$$1 - \varepsilon_w = \varepsilon; \tag{11b}$$

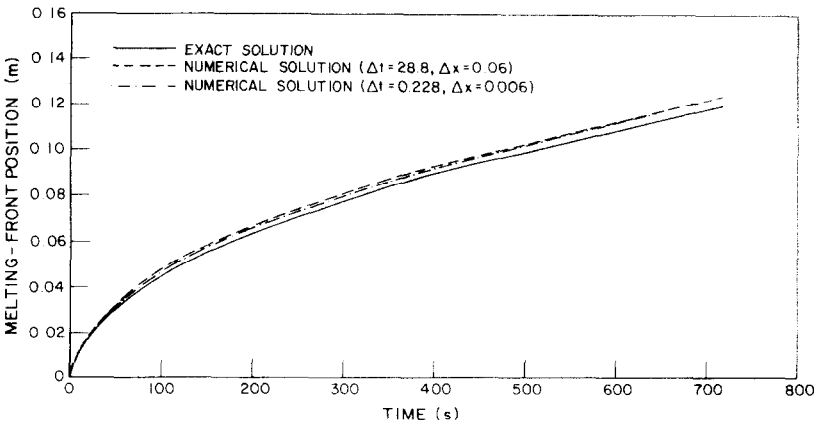

FIG. 2. Comparison of melting front position using exact [10] and numerical solutions of the Stefan model.

liquid continuity

$$\frac{\partial}{\partial t}[(1-\varepsilon_w)\alpha_l] = -(1-\varepsilon_w)\dot{m}/\rho_l; \tag{12}$$

vapor momentum

$$(1-\varepsilon_w)\alpha_g V^g = -\left(\frac{K_g}{\mu_g}\right)\frac{\partial P}{\partial x}; \tag{13}$$

mixture energy

$$\rho C_{pm}\frac{\partial T}{\partial t} + (1-\varepsilon_w)\alpha_g\rho_g C_{pg} V^g \frac{\partial T}{\partial x} = \frac{\partial}{\partial x}\left(K_e\frac{\partial T}{\partial x}\right) - (1-\varepsilon_w)\dot{m}\Delta H_v. \tag{14}$$

The volume fraction of vapor and liquid are constrained to add up as

$$\alpha_g + \alpha_l = 1. \tag{15}$$

The above equations derived by Lyczkowski [6] are based on the following assumptions:

(1) Heat transfer between the coal and the two-phase mixture is complete so that they are in a state of thermal equilibrium.

(2) Capillary forces are negligible.

(3) Vapor motion is slow enough so that all inertial terms may be dropped.

(4) The liquid does not move and so $V^l = 0$.

(5) Wall friction and pressure work terms are unimportant.

(6) The accumulation of mass of vapor is negligible compared to liquid.

We feel the assumption of negligible capillarity can be justified based on observations that many large cracks form probably caused by thermal and drying induced stresses [16, 17]. Capillarity could be included in the model as suggested by Lyczkowski [6].

The boundary and initial conditions for temperature are the same as the Stefan model and are given by equations (2)–(4).

The additional initial and boundary conditions are given by

$$a_g(0, x) = 0, \tag{16}$$

$$V^g(0, x) = 0, \tag{17}$$

$$\dot{m}(0, x) = 0, \tag{18}$$

$$\alpha_g(t, \infty) = 0. \tag{19}$$

There are six unknowns ρ_g, α_l, T, P, $\dot{m}$, and V^g, and five equations, equations (11)–(15), since μ_g, K_g, ρ_l, ε_w, K_e, C_{pm}, and ΔH_v are assumed to be known. To solve this problem, one additional assumption must be made. Experimental data for coal [1, 8, 9] and wood drying [16, 17] suggest the assumption that the saturation temperature is not a function of pressure. This may be possible if the pressure build up is small because of the formation of large cracks and fissures which allow the steam to flow easily [17]. The pressure build up has been measured in wood dowels (which have a tighter structure than Western coal) heated at a heat flux of 2 cal cm^{-2} s^{-1} (8.3×10^4 J m^{-2} s^{-1}) to be less than 0.3 atm [16]. We shall discuss the effect of permeability on pressure in Section 7.

An explicit finite-difference staggered-mesh [18] numerical scheme is used as shown in Fig. 3. The fundamental variables $P, T, \dot{m}$, and α_g are computed and defined at the center of each node j. The phase velocity V^g is computed and defined at the cell edges or junctions denoted by $(j \pm \frac{1}{2})$ for node j and denoted by $(V^g)_{j\pm 1/2}$.

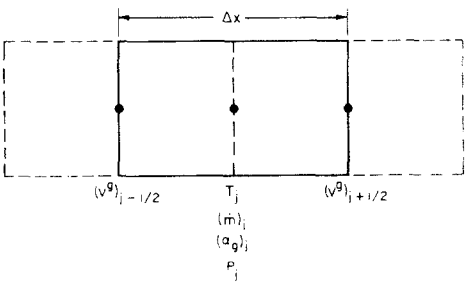

FIG. 3. Interior finite-difference mesh for two-phase model.

The indices $j \pm \frac{1}{2}$ are replaced inside the scheme by the integers j and $j+1$, where j is a volume number. In the description which follows, when fundamental nodal values are needed at junctions they are linearly averaged. The same applies for the junction velocity needed at cell centers.

The volume fraction α_g (or α_l) in the two-phase model replaces the distinct liquid–vapor interface in the Stefan model. The two-phase model assumes liquid and vapor to coexist locally in a representative control volume: $1 > \alpha_g > 0$ in the two-phase region, $\alpha_g = 1$ in the single-phase vapor region, and $\alpha_g = 0$ in the single-phase liquid region.

In the single-phase liquid and vapor regions, the phase change rate $\dot{m} = 0$ and therefore, some modifications of equations (11)–(14) are necessary for numerical computation purposes. In the two-phase region, liquid is continuously vaporized, and because the mass transfer rate $\dot{m} \neq 0$, it becomes much more difficult to solve the problem. The resolution of this difficult problem has been investigated by Solbrig *et al.* [18] and Lyczkowski and Solbrig [19] using two-phase unequal velocity equal temperature (UVET) and unequal velocity unequal temperature (UVUT) numerical schemes. As we mentioned earlier, the experimental data show that the temperature in the two-phase region remains essentially at a constant saturation value. This observation provides considerable simplification. Once the temperature in the single-phase liquid region reaches the saturation value for any finite-difference control volume, it is considered to be in the two-phase region. As time goes on, the volume fraction of vapor is allowed to change from 0^+ to 1^-, but the temperature will remain at the saturation temperature T_{vap} until $\alpha_g = 1$.

Now the problem is to determine the value of α_g for each node in the two-phase region. To determine α_g from equation (11), we must know $\dot{m}$ first. One way to get $\dot{m}$ is to assume an arbitrary value of $\dot{m}$ and then iterate using equations (11), (12), and (14) until convergence occurs. We used this method but found the convergence rate to be extremely slow. Another method to get $\dot{m}$ is by forming the difference in temperature calculated with and without the evaporation rate term. Since we already know that the temperature in the two-phase region is at saturation value T_{vap}, compute the temperature T_j^{n+1} for the next time step assuming no vaporization occurs. If it is above the saturation temperature and it is still in the two-phase region, the differences can only be caused by the evaporation term as long as Δt is chosen sufficiently small as discussed in Section 8. The procedures described can be summarized as follows:

(1) evaluate $\dot{m}$ from $\dot{m} \simeq -((T_j^{n+1} - T_{vap})/\Delta t) \times \rho C_{pm}/(\varepsilon \Delta H_v)$,

(2) calculate α_l from equation (12) and hence α_g,

(3) calculate $\rho_g V^g$ from equation (11),

(4) substitute these values into equation (14) to solve for T,

(5) solve for the pressure using equation (13).

The finite-difference approximations of equations (11)–(14) can be written as

$$\frac{(\varepsilon\alpha_l)^{n+1} - (\varepsilon\alpha_l)_j^n}{\Delta t} = -\varepsilon \dot{m}_j^n / \rho_l, \tag{20}$$

$$\frac{(\varepsilon\alpha_g \rho_g V^g)_{j+1/2}^n - (\varepsilon\alpha_g \rho_g V^g)_{j-1/2}^n}{\Delta x} = \varepsilon \dot{m}_j^n, \tag{21}$$

$$-\frac{K_g}{\mu_g}\left(\frac{P_{j+1}^n - P_j^n}{\Delta x}\right) = (\varepsilon\alpha_g V^g)_{j+1/2}^n, \tag{22}$$

$$(\rho C_{pm})_j^n \left(\frac{T_j^{n+1} - T_j^n}{\Delta t}\right) + (\varepsilon\alpha_g \rho_g V^g C_{pg})_{j+1/2}^n \left(\frac{T_{j+1}^n - T_j^n}{\Delta x}\right) = \frac{(K_e^n)_{j-1/2}(T_{j-1}^n - T_j^n) - (K_e^n)_{j+1/2}(T_j^n - T_{j+1}^n)}{(\Delta x)^2} - \varepsilon \Delta H_v \dot{m}_j^n, \tag{23}$$

where

$$\rho C_{pm} = \varepsilon \rho_g C_{pg} \alpha_g + \varepsilon \rho_l C_{pl} \alpha_l + (1-\varepsilon)\rho_w C_{pw}, \tag{24}$$

and

$$(K_e)_{j\pm1/2}^n = K_{ed}\left[\frac{(\alpha_g)_j^n + (\alpha_g)_{j\pm1}^n}{2}\right] + K_{ec}\left[\frac{(\alpha_l)_j^n + (\alpha_l)_{j\pm1}^n}{2}\right]. \tag{25}$$

The effective thermal conductivities of dry and moist coal K_{ed} and K_{ec}, respectively, in equation (25) are weighted by volume fraction as suggested by Lyczkowski [6].

4. COMPARISONS WITH KASHIWA AND HARLOW'S COAL DRYING DATA

In this section, we compare our numerical results with Kashiwa and Harlow's experimental data for the drying of moist Western coal [9]. The physical situation in the experiment is as follows.

A subbituminous coal sample 3.86 cm in diameter, 8.0 cm long is initially at room temperature and rapidly heated by electrical resistance to a temperature thereafter controlled at 200°C. Thermocouples are embedded in the sample along its length. The physical properties of this experiment are [9]:

microscopic density of water
$= 10^3$ kg m^{-3}
permeability of coal
$= 1.0$ md $= 9.86 \times 10^{-18}$ m^2
viscosity of vapor
$= 1.27 \times 10^{-5}$ Pa s
microscopic density of dry coal
$= 1.3 \times 10^3$ kg m^{-3}
density of insulation
$= 9.1$ kg m^{-3}
specific heat of water
$= 4.0 \times 10^3$ J kg^{-1} K^{-1}
specific heat of coal
$= 1.0 \times 10^3$ J kg^{-1} K^{-1}

specific heat of insulation
$= 2.0 \times 10^3$ J kg^{-1} K^{-1}
thermal conductivity of saturated coal
$= 0.8$ W m^{-1} K^{-1}
thermal conductivity of dry coal
$= 0.42$ W m^{-1} K^{-1}
thermal conductivity of insulation
$= 0.03$ W m^{-1} K^{-1}
heat of vaporization of water
$= 2.1 \times 10^6$ J kg^{-1}
saturation temperature of water at test altitude
$= 94$°C
local volume fraction of water
$= 10\%$.

We used the value of permeability of 1.0 md (9.8×10^{-18} m^2) which is in the range of dry coal and char [20].

We calculated the temperature distribution in 1-D Cartesian coordinates using the Stefan and two-phase models. The radial heat loss is assumed neglected because of the fiberglass insulation. The boundary condition at the heating surface is specified at a constant experimental temperature of 200°C. The second physical boundary condition at the opposite end is uncertain. Kashiwa and Harlow [9] report that the second (cold) surface "was exposed to a water reservoir whose temperature was controlled by a heater responsive to a buckling thermocouple pair, such that its temperature closely followed that of the coal 0.4 cm from the coal–water interface". Neither the reservoir water flow rate nor the temperature nor the heat transfer coefficient between coal and water were reported. Our treatment is to extend the original 8 cm length by different lengths L. The heat loss to the reservoir water in the system is simulated by the temperature rise in the extended region.

Figures 4 and 5 are the plots of the temperature profiles at two different times using $\Delta x = 0.2$ cm and $\Delta t = 0.4$ s. The two-phase model results match the experimental temperature profiles much more accurately than the Stefan model. Since we did not consider the radial heat loss from insulation, this could be one reason for the higher predicted temperature in the dried coal region. Another factor that may cause the higher predicted temperature in the dried coal region is the porosity change due to shrinkage and cracking during drying. A problem we encountered was the inconsistency between the reported moisture and porosity. Porosity in coal is quite difficult to measure accurately because of the presence of micropores, shrinkage, and cracking.

The reported moisture content of Kashiwa and Harlow's experiment is 12 wt. % from a proximate analysis. If we consider the dry coal and wet coal to have the same volume, we discover only 68 kg of water can fit inside the reported pore volume of 10% for 1000 kg of moist coal.

There are several ways to resolve this discrepancy. The first is to change the reported water density due to the presence of impurities. However, we discover the value would have to be 1.8×10^3 kg m^{-3} which is unrealistically high. We could also add some micropore volume. We would find that there would have an additional micropore volume fraction of 0.058 for a total volume fraction of 0.152. We could also consider this extra porosity as being due to shrinkage. Westmoreland and Dickerson found that Texas lignite shrinks $8.4 \pm 3\%$. We decided to reduce the reported moisture content to 6.8% accepting the reported 10% porosity. This corresponds to 100% saturation.

In the saturated coal region, the predicted temperature can go either higher or lower than the experimental data depending on the second boundary condition uncertainty. We did some comparisons using different extended lengths L as shown in Figs. 6 and 7.

From Fig. 6 at $t = 4.0 \times 10^3$ s, an extended length $L = 10$ cm caused the results to be a little closer to the experimental data. $L = 15, 25$, and 30 cm yield the same results, all somewhat higher than $L = 10$ cm. As time goes on a longer extended length is needed for the calculations to agree with the data as shown in Fig. 7.

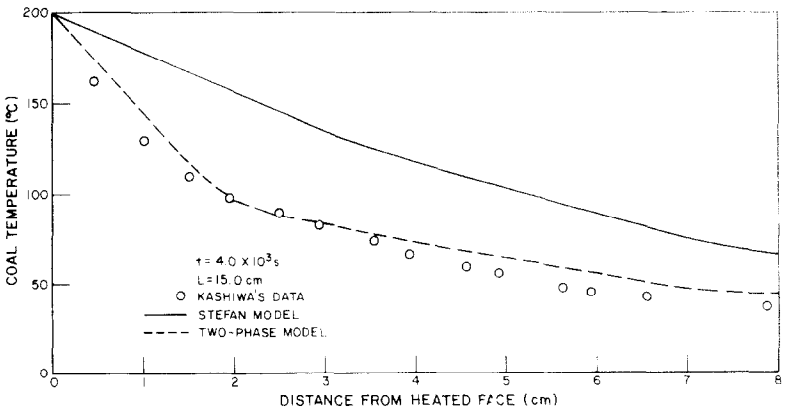

FIG. 4. A comparison of Stefan and two-phase models with Kashiwa and Harlow's experimental data at 4.0×10^3 s.

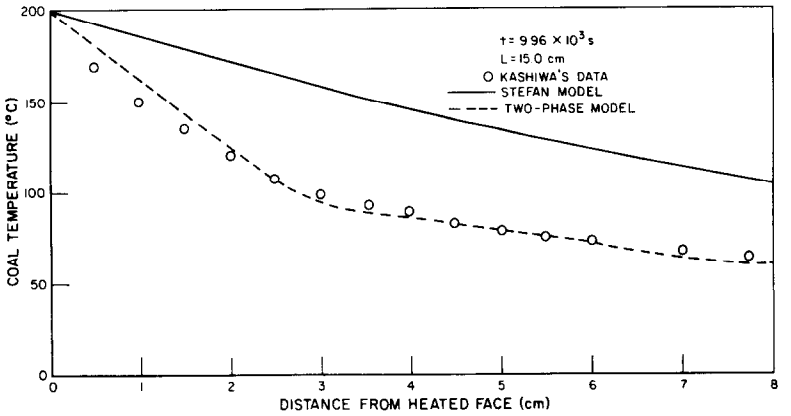

FIG. 5. A comparison of Stefan and two-phase models with Kashiwa and Harlow's experimental data at 9.96×10^3 s.

This effect can be explained by the penetration theory—the longer the time, the larger the influence of the heating surface on the distance. We estimate that our calculations have about 5% deviation based on our convergence study.

There were no moisture distributions reported in the experiment and so none are reported here.

5. COMPARISON WITH WESTMORELAND AND DICKERSON'S EXPERIMENTAL DATA

Westmoreland and Dickerson [8] used Wilcox lignite in their experiment. Instead of a constant heating surface temperature as in Kashiwa and Harlow's experiment, they used a temperature-programmed furnace to keep the heating surface temperature increasing at a constant rate of 3 K min^{-1} until a predetermined maximum was reached. The system was purged with argon and after a constant flow rate of purged gas was established, heating was started.

We calculated the temperature distribution in 1-D axisymmetric coordinates using both the Stefan and two-phase models. The physical properties we used were [8]:

radius of coal sample
$= 7.62$ cm
thermal conductivity in dried coal region
$= 0.14$ W m^{-1} K^{-1}
thermal conductivity in saturated coal region
$= 0.37$ W m^{-1} K^{-1}
porosity of coal
$= 0.3$
density of water
$= 1.0 \times 10^3$ kg m^{-3}
density of vapor
$= 5.98 \times 10^{-1}$ kg m^{-3}
density of dried coal
$= 1.33 \times 10^3$ kg m^{-3}
saturation temperature of water
$= 373$ K
heat capacity of water
$= 4.213 \times 10^3$ J kg^{-1} K^{-1}
heat capacity of vapor
$= 2.059 \times 10^3$ J kg^{-1} K^{-1}

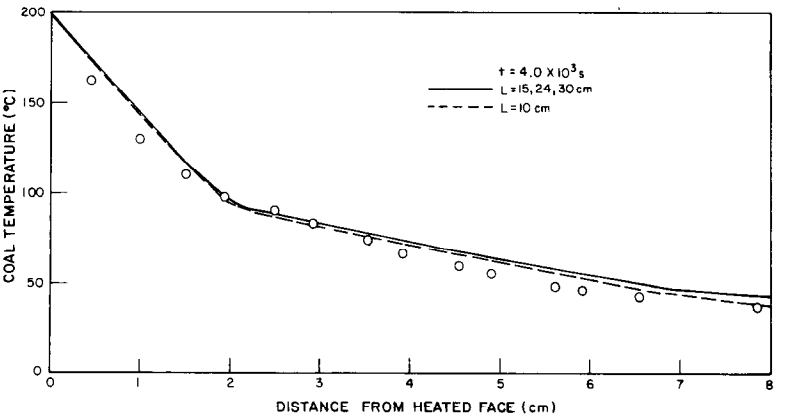

FIG. 6. The effect of simulated length on the temperature distribution in Kashiwa and Harlow's experiment at 4.0×10^3 s.

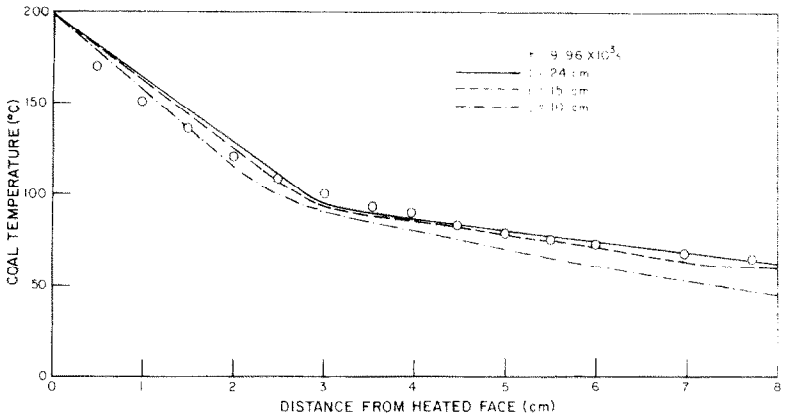

FIG. 7. The effect of simulated length on the temperature distribution in Kashiwa and Harlow's experiment at 9.96×10^3 s.

heat capacity of coal
$= 1.6 \times 10^3$ J kg^{-1} K^{-1}
viscosity of vapor
$= 1.27 \times 10^{-5}$ Pa s
permeability of coal
$= 9.86 \times 10^{-18}$ m^2 (1 md).

The coal was assumed to be saturated with water.

The effect of temperature on these properties was neglected. The thermal conductivity of dry coal in Westmoreland and Dickerson's experiment was chosen as 0.14 W m^{-1} K^{-1}, which is adequate in the temperature range of 410–570 K and 30% porosity. The specific heat of dry coal used was 1.6 J kg^{-1} K^{-1} which is actually the value obtained at 500 K. Also, the effects of temperature and pressure on vapor density, viscosity, specific heat, etc. are all neglected. These factors can cause a slight difference on the temperature distribution especially in the dry coal region, which is more sensitive than the wet coal region.

Figures 8–11 plot coal temperature against distance at different times by using $\Delta t = 0.29$ s and $\Delta x = 0.0762$ cm. We can see both models agree well with experimental data in the saturated coal region. In the dried coal region, the two-phase model predicts the temperature much better than the Stefan model does up to a surface temperature of 600°C. At surface temperatures over 600°C, the net effect of pyrolysis and steam self-gasification reactions apparently cause the drying region to move faster than the calculated results, ignoring chemical reactions, as can be seen in Fig. 11.

Once again, no moisture distributions were reported in the experiment and so none are reported here.

6. HEATING RATE STUDY

From the previous two sections, we can clearly see that the two-phase model is better than the Stefan model for predicting temperature distributions during coal drying. The basic difference between these two models is the heat transfer mechanism. In the two-phase model, both conductive and convective heat transfer are considered, whereas in the Stefan model, only conductive heat transfer is involved. In the problem of solid–liquid phase change, the Stefan model is adequate as proved by previous workers because there is not much convective heat transfer involved. In the case of liquid–vapor phase change, a lot of steam is produced which flows outward opposite to the drying

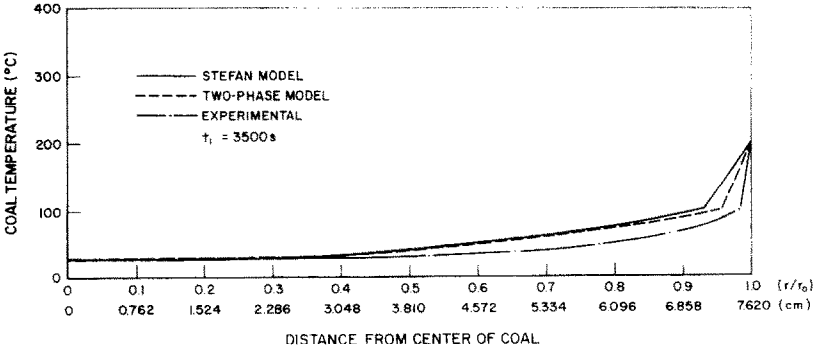

FIG. 8. A comparison of Stefan and two-phase models with Westmoreland and Dickerson's experimental data at 3500 s.

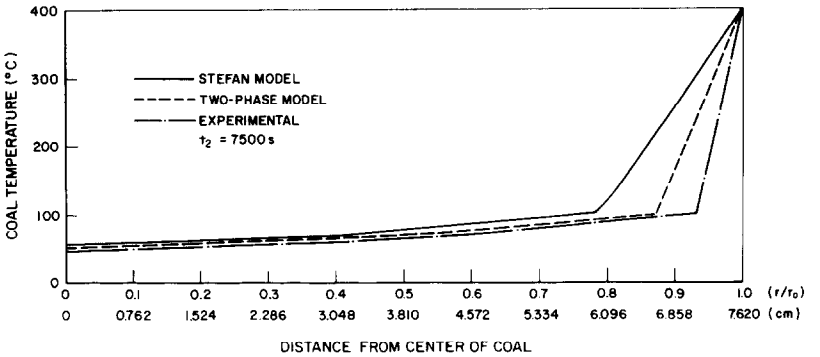

FIG. 9. A comparison of Stefan and two-phase models with Westmoreland and Dickerson's experimental data at 7500 s.

front motion because of the internally generated pressure build up. This steam flow carries large amounts of energy out of the system, and hence, decreases the local temperature. This is shown clearly in Figs. 4 and 5 and Figs. 8 and 11. The two-phase model usually predicts a lower temperature than the Stefan model.

Figures 12–14 are the comparisons of these two models at three different heating rates using Westmoreland and Dickerson's experiment. We can see that the higher the heating rate, the larger the difference in predicted temperatures. They differ mainly because of the higher heat flux producing more steam. The convective term is missing in the Stefan model, and hence, the drying rate is consistently faster than the two-phase model. This term acts as a transpiration cooling mechanism bringing cooler steam into the hotter dried coal region. At a heating rate of 0.6 K min^{-1}, these two models basically agree as shown in Fig. 12. Part of the disagreement may be due to variation in the physical properties.

7. PERMEABILITY STUDY

As we mentioned in Section 3, our calculations are based on the assumptions: (1) the saturation temperature will not be affected by the pressure build up; and (2) no shrinkage during the heating process. We examined these two assumptions by computing the pressure using different permeabilities. Figure 15 shows that the maximum pressure is at the drying front, and the lower the permeability, the larger the pressure build

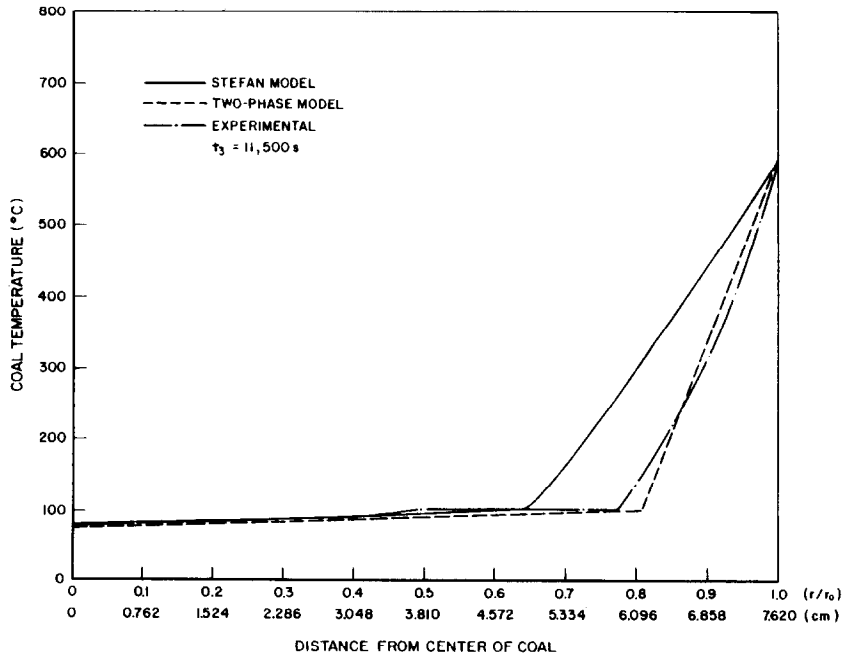

FIG. 10. A comparison of Stefan and two-phase models with Westmoreland and Dickerson's experimental data at 11 500 s.

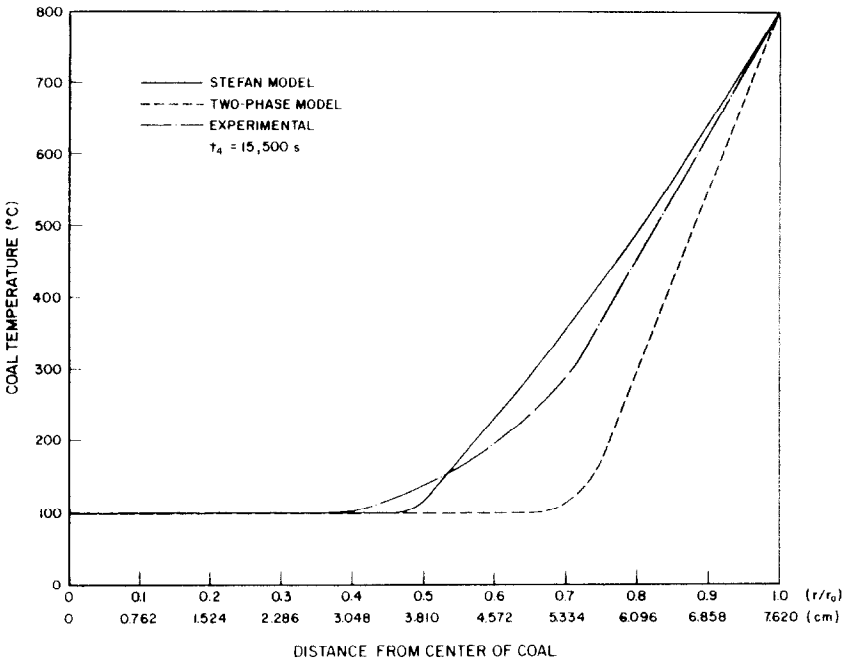

FIG. 11. A comparison of Stefan and two-phase models with Westmoreland and Dickerson's experimental data at 15 500 s.

up. As can be seen from Fig. 15 and Table 1, permeability over 9.86×10^{-19} m^2 (0.1 md) causes an increase of pressure less than about 1.5×10^4 Pa which causes the saturation temperature to change less than 3.5°C. The drying rate is not affected by the permeability variation over the range used. It is primarily a function of the heating rate.

8. SENSITIVITY STUDY

To our knowledge, there is no stability criterion for explicit finite-difference solution of the complex mixture energy equation (14) coupled with equations (11)–(13a). To choose suitable Δt and Δx, we assumed the stability criterion that the ratio of $(\alpha \Delta t)/(\Delta x)^2$ must be less than 0.5, because the mixture energy equation is reduced to a simple diffusion equation in the single-phase liquid region. We used the ratio of 0.3 at first, but we found the solution to be unstable in the single-phase vapor region because of the appearance of the convective term. Different values of this ratio were tested. Finally, we chose a ratio of about 0.08. In the two-phase region, the situation is even more complex. To get a reasonable estimate of $\dot{m}$, Δt is kept small so no single-phase liquid node changes to a single-phase vapor node within one time step. Figure 16 shows a

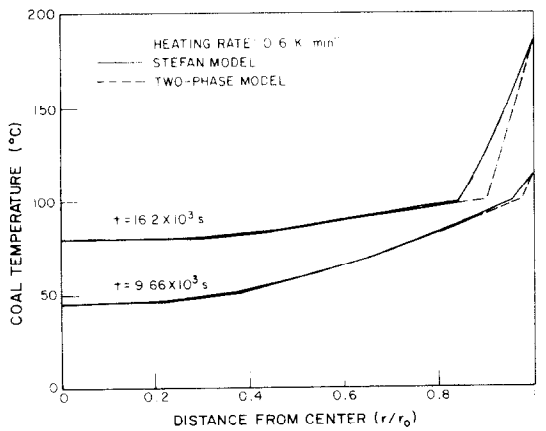

FIG. 12. A comparison of Stefan and two-phase models at a heating rate of 0.6 K min^{-1}.

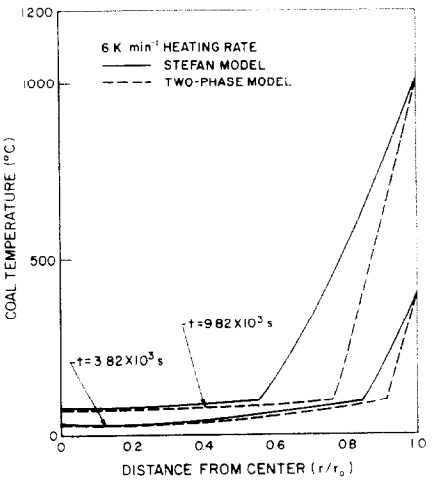

FIG. 13. A comparison of Stefan and two-phase models at a heating rate of 6 K min^{-1}.

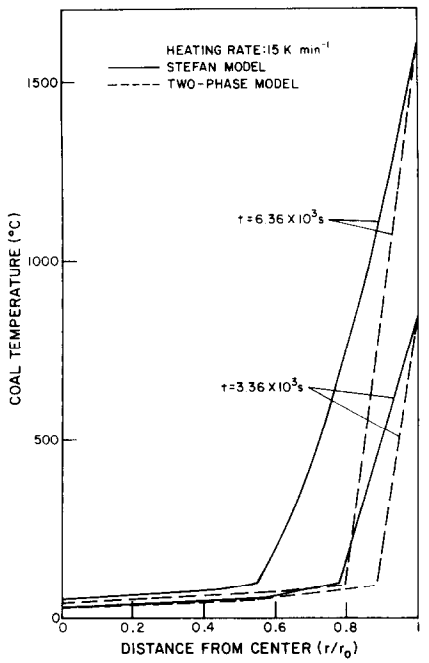

FIG. 14. A comparison of Stefan and two-phase models at a heating rate of 15 K min^{-1}.

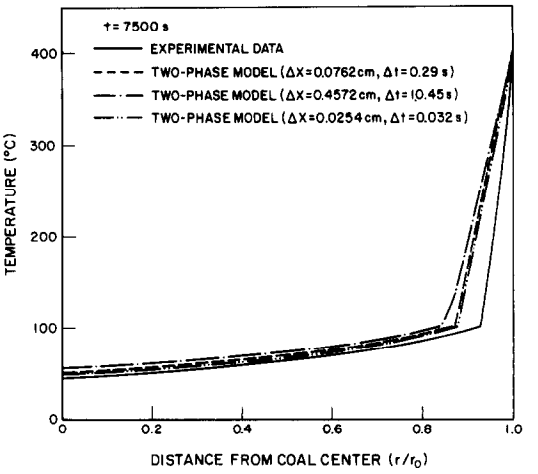

FIG. 16. Comparison of two-phase model using different Δx and Δt.

comparison with Westmoreland and Dickerson's experimental data using different Δx's and Δt's. We can see these results are quite close. Part of the deviation may be due to the estimation of $\dot{m}$.

Because of the error probability involved in the measurements of K_e, we tested our numerical scheme to see how sensitive it was to the variation in K_e. Figure 17 plots temperature distribution against distance at different K_e's which are chosen $\pm 20\%$ from the reported data [8]. We conclude that the effect of K_e on generating temperature distributions in our range of study is about $\pm 10\%$.

9. CONCLUSIONS

Comparisons with experimental temperature data reveal that the two-phase model is more accurate than the Stefan model in dealing with coal drying for heating rates typical for underground coal gasification. From our calculations, we did not see the existence of a temperature plateau between the wet coal region and the dry coal region but just a single two-phase node. The temperature of adjacent points in the wet coal region approach the saturation value, but never reach it until the two-phase point becomes pure vapor phase. This result can be explained from the mixture energy equations. If a plateau exists, there is no temperature gradient, so the conduction and convection terms in equation (3) vanish. Further evaporation of liquid water will cause the temperature in the two-phase region to decrease. If we consider the influence of

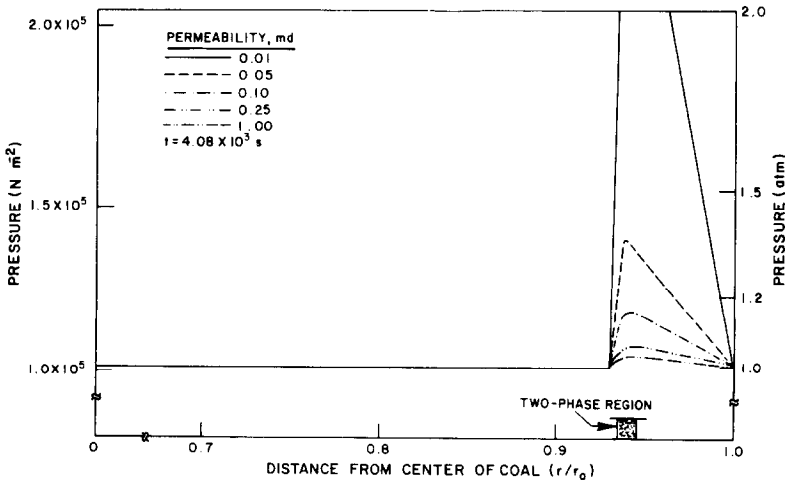

FIG. 15. The effect of permeability on the maximum pressure build up.

Table 1. Maximum build up and saturation temperature change for different permeabilities for heating rate of 3 K min^{-1}

(m^2)	Permeability (md)	Maximum pressure (Pa)	T_{vap} (°C)	$T_{vap} - 100$ (°C)
9.86×10^{-18}	(1)	1.04×10^5	100.8	0.8
2.47×10^{-18}	(0.25)	1.07×10^5	101.6	1.6
9.86×10^{-19}	(0.10)	1.17×10^5	103.5	3.5
4.93×10^{-19}	(0.05)	1.38×10^5	108.8	8.8
9.86×10^{-20}	(0.01)	2.63×10^5	128.8	28.8

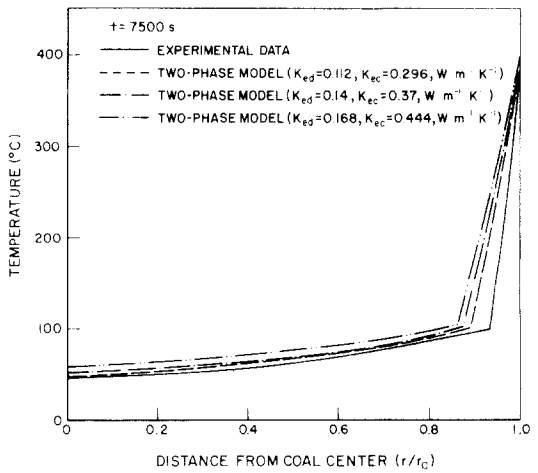

FIG. 17. The effect of effective thermal conductivity on the calculated results.

pressure build up on saturation temperature, a plateau is possible, but it is not absolutely flat.

In summary, the two-phase model provides us with a very acceptable method to deal with coal drying, the Stefan model does not. Based on our comparisons, several conclusions can be drawn:

(1) The Stefan model is accurate only for surface heating rates less than 0.6 K min^{-1}.

(2) As surface heating rates reach 3 K min^{-1} or higher, the two-phase model is more accurate because of the steam flow caused by $\dot{m}$.

(3) The steam flow rate is primarily a function of the surface heating rate and is not affected by the permeability.

(4) The two-phase model is good for temperatures less than 600°C.

(5) Our calculation is accurate for a maximum pressure rise less than 1.17×10^5 Pa (0.15 atm).

Acknowledgements—The funding for this work was provided for in part by a subcontract from the Lawrence Livermore National Laboratory (LLNL). Special thanks are due to Dr Douglas R. Stephens, Manager of LLNL Underground Coal Gasification Project, for personally encouraging this work as 'cross-cutting' technology research. Dr Charles B. Thorsness of LLNL provided technical coordination and additional encouragement and helped to keep the research focused. We thank the Institute of Gas Technology (IGT) for fellowship support, (Y.-T.C.), and for providing research facilities. We also thank IGT's Computer Department for their cooperation. Mrs L. Courtney of IGT typed the M.S. thesis which formed the basis of this paper, and Miss Brenda Wright of Argonne National Laboratory typed the manuscript.

REFERENCES

1. J. H. Campbell, Pyrolysis of subbituminous coal in relation to in-situ coal gasification, *Fuel* **57**(4), 217–224 (1978).
2. T. H. Tsang and T. F. Edgar, Modeling of drying and pyrolysis during underground coal gasification, paper presented at the AIChE National Meeting, Houston, Texas, 1–4 April (1979).
3. W. B. Van Arsdel, Drying phenomena, in *Food Dehydration* (edited by Van Arsdel *et al.*), Vol. 1. AVI, Westport, Connecticut (1973).
4. R. W. Peck, K. C. Vyas and R. Toci, Capillary theory applied to drying, *A.I.Ch.E. Symp. Ser. No. 163*, **63** (1973).
5. S. Whitaker, Simultaneous heat, mass, and momentum transfer in porous media: a theory of drying, in *Advances in Heat Transfer* (edited by J. P. Hartnett and T. F. Irvine, Jr.), Vol. 15, pp. 119–203. Academic Press, New York (1977).
6. R. W. Lyczkowski, The development of a mechanistic theory for drying of porous media using two-fluid flow theory, in *Multiphase Transport Fundamentals, Reactor Safety, Applications* (edited by T. N. Veziroglu), Vol. 5, pp. 2289–2318. Hemisphere, Washington, DC (1980).
7. M. Cross, R. D. Gibson and R. W. Young, Pressure generation during the drying of a porous half-space, *Int. J. Heat Mass Transfer* **22**, 47–50 (1979).
8. P. R. Westmoreland and L. S. Dickerson, Pyrolysis of Texas lignite, paper presented at the AIChE 86th National Meeting, Houston, Texas, 1–5 April (1979).
9. B. A. Kashiwa and F. H. Harlow, An investigation of simultaneous heat and mass transfer in subbituminous coal, *Proc. 15th Intersociety Energy Conversion Engng Conf.*, Vol. 2, pp. 1311–1314. Am. Inst. Aeronautics and Astronautics (1980).
10. H. S. Carslaw and J. C. Jaeger, *Conduction of Heat in Solids* (2nd edn.), pp. 282–296. Oxford University Press, Oxford (1959).
11. W. D. Murray and F. Landis, Numerical and machine solutions of transient heat conduction problems involving melting or freezing, Part I, *Trans. Am. Soc. Mech. Engrs*, Series C, *J. Heat Transfer* **81**, 106–112 (1959).
12. G. S. Springer and D. R. Olson, Method of solution of axisymmetric solidification and melting problem, ASME Paper 62-WA-246 (1962).
13. A. Lazaridis, A numerical solution of the multidimensional solidification (or melting) problem, *Int. J. Heat Mass Transfer* **13**, 1459–1477 (1970).
14. W. W. Yuen and A. M. Kleinman, Application of a variable time-step finite difference method for the one-dimensional melting problem including the effect of subcooling, *A.I.Ch.E. Jl* **26**(5), 828–832 (1980).
15. Y.-T. Chao, Numerical studies of coal drying with applications to underground coal gasification, M.S. thesis, Gas Engineering Dept., Illinois Institute of Technology, Chicago, Illinois, December (1981).

16. E. J. Kansa, H. E. Perlee and R. F. Chaiken, Mathematical model of wood pyrolysis including internal forced convection, *Combust. Flame* **29**, 311–324 (1977).
17. E. J. Kansa, A model of drying: drying and pyrolysis of solid fuel at fire intensity conditions, in *Drying 82*, pp. 25–31. Hemisphere, Washington, DC (1982).
18. C. W. Solbrig, G. A. Mortensen and R. W. Lyczkowski, An unequal phase velocity unequal phase temperature theory applied to two-phase blowdown from a horizontal pipe, in *Proc. 25th Heat Transfer and Fluid Mechanics Institute*, pp. 60–67. Stanford University Press, Stanford, California (1976).
19. R. W. Lyczkowski and C. W. Solbrig, Calculation of the governing equations for a seriated unequal velocity equal temperature two-phase continuum, *A.I.Ch.E. Jl* **26**(1), 89–97 (1980).
20. E. J. Kansa and H. E. Perlee, A transient dust-flame model: application to coal-dust flames, *Combust. Flame* **38**, 17–36 (1980).

COMPARAISON DU MODELE DE STEFAN AVEC CELUI DU SECHAGE DIPHASIQUE DU CHARBON

Résumé—Le modèle de Stefan a été fréquemment proposé pour décrire le sèchage rapide et fortement non isotherme des milieux poreux. En particulier, il a été utilisé pour analyser le sèchage des charbons et des lignites qui contiennent jusqu'à 40% d'eau, la grande part n'étant pas liée. Le modèle de Stefan peut être approprié pour le mécanisme de gel mais il peut être défaillant pour les mécanismes dans lesquels beaucoup de vapeur est produite dans le matériau poreux et que des écoulements vers l'extérieur se produisent à cause des pressions internes créées. Récemment, le premier auteur a développé un modèle mécanique appelé modèle diphasique pour élargir la théorie du sèchage. L'objet de cet article est: (1) de comparer le modèle de Stefan et celui du sèchage diphasique an analysant les expériences de sèchage de lignite et de charbon; et (2) de déterminer le domaine des flux thermiques pour lequel le modèle de Stefan est acceptable. Ce texte est, à notre connaissance, le premier à fixer l'aptitude du modèle de Stefan pour décrire le sèchage du charbon.

EIN VERGLEICH DES STEFAN-MODELS MIT DEM ZWEIPHASEN-MODELL ZUR KOHLETROCKNUNG

Zusammenfassung—Das Stefan-Modell wurde vielfach verwendet, um die stark nichtisotherme schnelle Trocknung von porösen Stoffen zu beschreiben. Im besonderen wurde es benutzt, um die Trocknung von "Western Coals" und Braunkohle, die bis zu 40% Wasser meist in ungebundener Form enthalten, zu untersuchen. Das Stefan-Modell mag für Gefriervorgänge tauglich sein, aber es versagt bei Vorgängen, bei denen innerhalb des feuchten, porösen Gutes viel Dampf gebildet wird und durch innere Druckerhöhung nach außen gerichtete Strömungen entstehen. Der erstgenannte Autor hat kürzlich ein mechanistisches Modell zum dynamischen Feuchtetransport, das sogenannte Zweiphasenmodell, entwickelt. Dieses Modell soll das bestehende Manko beseitigen und die Theorie der Trocknung sinngemäß erweitern. Das Ziel dieser Arbeit ist, (1) das Stefan-Modell und das Zweiphasentrocknungsmodell anhand von Braunkohleblock-Pyrolyse und Moorkohle-Trocknungsexperimenten zu vergleichen; und (2) den Bereich der Heizraten, in denen das Stefan-Modell anwendbar ist, zu bestimmen. Diese Arbeit ist nach unserer Kenntnis die erste, die den Einsatzbereich des Stefan-Modells zur Beschreibung der Kohletrocknung qualitativ abschätzt.

СРАВНЕНИЕ МЕЖДУ МОДЕЛЬЮ СТЕФАНА И ДВУХФАЗНОЙ МОДЕЛЬЮ СУШКИ УГЛЯ

Аннотация—Для описания сильно неизотермического быстропротекающего процесса сушки пористых сред часто используется модель Стефана. В частности, эта модель применялась для анализа сушки западных углей и лигнитов, содержащих до 40% воды, большей частью находящейся в несвязанном состоянии. Модель Стефана может также использоваться для описания процессов замораживания, но может оказаться непригодной для процессов, при которых внутри влажного пористого материала образуется большое количество пара, выходящего наружу под действием образующегося внутри материала давления. Для устранения этого недостатка первым автором статьи была разработана модель динамики влаги, названная двухфазной моделью, которая существенно пополнила теорию сушки. Данная работа была выполнена с целью: (1) сравнить модель Стефана с двухфазной моделью сушки на основе анализа пиролиза лигнитового блока и экспериментального исследования сушки битумного угля; и (2) определить диапазон скоростей нагрева, при которых можно использовать модель Стефана. Насколько известно авторам, эта работа является первой, в которой предпринята попытка количественного определения адекватности модели Стефана для описания сушки угля.